

Junctophilin-2 physically interacts with ryanodine receptor type 2 for peripheral coupling of mouse cardiomyocytes

Tianxia Luo

Zhengzhou University

Ningning Yan

Zhengzhou University

Mengru Xu

Zhengzhou University

Fengjuan Dong

Zhengzhou University

Qian Liang

Zhengzhou University

Ying Xing

Zhengzhou University

Hongkun Fan (✉ fanhk@zzu.edu.cn)

Zhengzhou University <https://orcid.org/0000-0002-2480-2636>

Research

Keywords: junctophilin2; ryanodine receptor type 2; peripheral coupling; cardiac SR membrane vesicles; endoplasmic reticulum; cardiomyocyte

Posted Date: April 6th, 2020

DOI: <https://doi.org/10.21203/rs.3.rs-20484/v1>

License: © ⓘ This work is licensed under a Creative Commons Attribution 4.0 International License.

[Read Full License](#)

Abstract

Background: Ryanodine receptor type 2 (RyR2) mediate Ca²⁺ release from the endoplasmic and sarcoplasmic reticulum (ER and SR), which is involved in the peripheral coupling of mouse cardiomyocytes, and thereby plays an important role in cardiac contraction. Junctophilin-2 (JPH2, JP2) is anchored to the plasma membrane (PM) and membranes of the ER and SR, and modulates intracellular Ca²⁺ handling through regulation of RyR2. However, the potential RyR2 binding region of JPH2 is poorly understood. Methods: The interaction of JPH2 with RyR2 was studied using LC-MS/MS, bioinformatic analysis, co-immunoprecipitation studies in cardiac SR vesicles. GST-pull down analysis was performed to investigate the physical interaction between RyR2 and JPH2 fragments. Immunofluorescent staining was carried out to determine the colocalization of RyR2 and JPH2 in isolated mouse cardiomyocytes. Ion Optix photometry system was used to measure the levels of intracellular Ca²⁺ transients in cardiomyocytes isolated from JPH2 knock down mice. Results: We report that (i) JPH2 interacts with RyR2 and (ii) the C terminus of the JPH2 protein can pull down RyR2 receptors. Confocal immunofluorescence imaging indicated that the majority of JPH2 and RyR2 proteins were colocalized near Z-lines. A decrease in the levels of JPH2 expression reduced the amplitude of Ca²⁺ transients in cardiomyocytes. Conclusions: This study suggests that the C terminus domain of JPH2 is required for interactions with RyR2 in the context of peripheral coupling of mouse cardiomyocytes, which provide a molecular mechanism for looking for Ca²⁺ - related diseases prevention strategies.

Introduction

Ryanodine receptors (RyRs) are a mediate Ca²⁺ release channel from stores of intracellular Ca²⁺ such as endoplasmic reticulum (ER/SR)[1–4]. Among RyRs, RyR1 is expressed in skeletal muscle, RyR2 is predominantly expressed in cardiac muscle, RyR3 is ubiquitously expressed in parotid acinar cells, central nervous systems, and skeletal muscles [2–4]. In striated muscle, activation of voltage-gated Ca²⁺ channels (VGCC) in the plasma membrane (PM) by membrane depolarization induces a much greater Ca²⁺ release from SR via RyR1 and RyR2, and induces muscle contraction[2, 3]. The process named Ca²⁺-induced Ca²⁺-release in cardiomyocytes occurs mainly in diad or peripheral coupling, and is associated with the formation of T-tubules invaginated in the PM and which are closely juxtaposed with a single terminal cistern of the ER/SR[2, 3]. Firm evidence indicates that Junctophilins (JPHs, JPs) interact with VGCC and RyRs to regulate Ca²⁺ homeostasis and help to induce excitation contraction coupling in muscles[5–8].

JPHs are proteins of a family of junctional membrane complex (JMC) located and facilitating contact between the PM and ER membrane in all excitable cells[9]. Skeletal muscles express both JHP1 and JPH2, cardiac muscles only express JPH2, JPH3 and JPH4 are mainly expressed across parts of the central nervous system[9, 10]. All JPHs contain eight membrane occupation and recognition nexus (MORN) domains which is able to interact with PM and are followed by an α helical region, a divergent region, and which includes C-terminal domain anchoring proteins located in the ER/SR[9, 11]. The mice with knocked out JPH2 do not survive and die in embryo phase due to heart failure (HF) caused by

decoupling of the excitation contraction, which indicates that JPH2 is essential for functional crosstalk between VGCC and RyR2 for proper functioning of the embryonic heart[9]. As JPH2 was down-regulated in cases of cardiomyopathy and HF, it was found that a subsequent induction of levels of overexpression of JPH2 corrected cardiac function for mice with early stage heart failure, inhibited SR Ca²⁺ leaks induced by RyR2[12, 13]. Quantitative single-molecule localization microscopy also indicated that colocalization between RyR2 and JPH2 in JPH2 knocked down cardiomyocytes was reduced. In contrast, for cases of induced overexpression of JPH2 in cardiomyocytes, there was colocalization of RyR2 with JPH2 at levels that were significantly increased[14]. However, the binding domain between JPH2 and RyR2 channel has not been fully elucidated.

In the present study, we sought to further examine the molecular regulation of RyR2 channel by JPH2 protein in the peripheral coupling of mouse cardiomyocytes, and to determine whether interaction sites were localized to the C terminus of JPH2 proteins.

Materials And Methods

Animals

We used 3-month-old mature C57BL/6 mice of both sexes obtained from Beijing Weitong Lihua Experimental Animal Technology, Limited, China (No. SCXK Jing 2012-0001). Ethics for animal care followed guidelines from the Committee on the Ethics of Animal Experiments of the University of Zhengzhou, China (No. SYXK-2010-0001). Procedures for experimental use of animals followed guidelines from the National Institutes of Health and Institution. All mice were group housed on 12 hr light/dark cycles with food and water available ad libitum.

Plasmids construction

Three GST-JPH2 fragment plasmids GST-JPH2-N1(aa1–253), GST-JPH2-N2 (aa216-350) and GST-JPH2-C (aa340-696) were subcloned into pGEX-4T-1 vector as previously described[15]. JP2-C cDNA was subcloned into pRyR2-IRES2 to generate RyR2 + JP2-C, a plasmid that contained JP2-C and RyR2 cDNA. Site-directed mutagenesis was used to construct the JP2 A405S mutation and the mutation were introduced into the pIRES2-RyR2 + JP2-C vector. The accuracy of the plasmids was verified using nucleotide sequencing.

Cardiac SR membrane vesicles isolation

Cardiac SR membrane vesicles were isolated using differential centrifugation as previously described[16, 17]. Mice were anaesthetized using chloralhydrate. Whole hearts were quickly removed by careful dissection and stored at -80 °C. Heart samples were minced and homogenized in a cold lysis buffer containing 0.25 M sucrose, 10 M Tris-HCl (pH 7.0), and 1 mM EDTA. Individual homogenates were centrifuged at 5000 g for 10 min. Supernatant was removed and samples were centrifuged at 40,000 g for 45 min. The resultant pellet representative of the SR vesicles was suspended in 0.6 M KCl solution

and centrifuged at 40,000 g for 45 min. The pellet was suspended in a cold lysis buffer and then stored at -80 °C until future use.

HEK293 cells transfection

HEK293 cells were transiently transfected at 70–80% confluency using Lipofectamine 2000(Invitrogen) along with the following cDNAs: pIRES2-RyR2 + JP2-C or pIRES2-RyR2 + JP2-Cmut plasmids, by following the manufacturer's instructions. Forty-eight hours after transfection, cells were solubilized for further experiments.

Western blot analysis

Protein was extracted from SR vesicles or transfected HEK293 cells lysate were separated by SDS-PAGE, and transferred to 0.45 µm polyvinylidene difluoride (PVDF) membranes (Millipore, Bedford, MA, USA). Membranes were blocked and incubated with primary antibodies specific to JPH2 (cat. no. PRS4919; diluted 1:300; Sigma) or antibodies specific to RyR2 (cat. no. MA3-916; diluted 1:600; Thermo Fisher Scientific) or antibodies specific to GAPDH (cat. no. G9545; diluted 1:1000; Sigma) at 4 °C overnight. Then, visually observed bands were incubated with HRP-conjugated secondary antibodies (Bio-Rad) and the products were examined for positive detections using ECL reagents (Thermo Fisher Scientific).

Co-immunoprecipitation

Solubilized SR vesicles or transfected HEK293 cells lysis were incubated with anti-JPH2 or RyR2 antibodies at 4 °C overnight, followed by incubation with protein A/G sepharose (Santa Cruz) for 6 h at 4 °C. Next, the beads were washed for 10 min with washing buffer, collected after each wash and resuspended in SR vesicle sample buffer by boiling for 5 min. Extracted precipitated proteins were used for SDS-PAGE separation and Coomassie blue staining described in steps below.

Protein Digestion and LC-MS/MS analysis

Immunoprecipitated complexes were separated using SDS-PAGE gradient (4%-8%-12%) followed by Coomassie-staining. The sectioned portion of each vertical lane from each gel was placed in Trypsin for digestion and peptide based extraction performed as previously described [18]. Every gel lane was chopped, destained using 25 mM NH_4HCO_3 and 50% acetonitrile, and was dried in a speedVac. Individual dessicated samples were added together to perform another gel-based digestion wherein we used a trypsin digestion buffer for 24 h at 37 °C. Peptides were extracted by using 60% acetonitrile and 5% trifluoroacetic acid solutions and identified by using LC-MS/MS and liquid chromatography quadrupole time-of-flight (LC-QqTOF) mass spectrometry (Waters). Tandem measurements of mass were obtained from the resultant raw files, and we used Mass lynx 4.0 software to identify and characterize peptide sequences. Identified proteins were submitted to the National Center of Biotechnology Information non-redundant Database (NCBIInr).

Functional categorization and network analysis

Proteins that were identified using LC-MS/MS analyses were screened by making comparisons to available published literature. The resultant selected proteins were submitted to Gene Ontology (<http://www.geneontology.org/>) for functional categorization. We used the string mapping tool (<http://www.string.embl.de/>) to analyze the levels of interaction between the different proteins.

GST pull-down assays

Construction of the GST-JPH2 fragment plasmids and implement of GST-pull down assays were performed in our previous study[15]. Briefly, plasmids were transformed into E. coli BL-21 (DE3), and were induced into samples by using 0.1 mM isopropyl- β -D-thiogalactoside (IPTG) at 20 °C with 40r overnight. The resultant immobilized GST, GST-JPH2-N1, GST-JPH2-N2, and GST-JPH2-C were incubated with the protein samples prepared from SR vesicles at 4 °C overnight. The pulldown complexes were eluted using elution buffer as part of the Pierce GST protein interaction pull-down kit. Eluted products were boiled for 5 min at 95 °C, and then analyzed by western blot analysis.

Single cardiomyocyte isolation

Single cardiomyocyte samples were prepared as described in a previous study[15]. After application of anesthesia using sodium pentobarbital, whole hearts from adult mice were rapidly dissected and washed with ice-cold Ca^{2+} -free modified Tyrode's solution (140 mM NaCl, 5.4 mM KCl, 1 mM MgCl_2 , 10 mM HEPES, and 10 mM glucose at pH 7.4). Each heart sample was cannulated and mounted onto a Langendorff perfusion system, perfused with a fresh enzyme solution (collagenase type II and protease) for 35 min, and then was subjected to a high- K^+ solution (120 mM potassium glutamate, 20 mM KCl, 1 mM MgCl_2 , 0.3 mM EGTA, 10 mM glucose, and 10 mM HEPES, adjusted to pH 7.4 with KOH) for 5 min. Single atrial and ventricular cells were isolated and kept within the high- K^+ solution before we undertook immunocytochemistry and measurements of Ca^{2+} transient.

Immunocytochemistry

Single atrial and ventricular cells were fixed in 4% paraformaldehyde for 30 min, treated with 0.4% Triton X-100 for 15 min, washed and incubated with anti-RyR2 antibody (dilution 1:100) and or anti-JPH2 antibody (dilution 1:100) at 4 °C overnight. Cells were incubated with FITC-conjugated goat anti-mouse antibody (dilution 1:250, Jackson Immuno Research) and or incubated with TRITC-conjugated goat anti-rabbit antibody (dilution 1:250, Jackson Immuno Research) for 1 h. An Olympus FV1000 confocal laser scanning microscopy was used to visualize the fluorescence signals (Japan).

JPH2 knockdown by RNA interference

Oligonucleotides encoding shRNAs (GTATGGTGATCTTGCTGAA) and a negative control shRNA (TTCTCCGAACGTGTCACGT) used for our study were previously successfully constructed. We applied a total dose of 1×10^9 PFU adenovirus with control siRNA and JPH2 siRNA by means of delivery into mice as previously described [15].

To determine quantitative levels of JPH2 and RyR2 mRNA expression, total RNA was isolated from infected myocardium using Trizol (Thermo Fisher Scientific) and was analyzed using Real-time PCR as described[19]. PCR primer used to detect levels of expression of JPH2, RyR2, and GAPDH were listed in Table1. Each primer sets were designed and synthesized by Shanghai Genechem Biotechnology, Shanghai, China. The relative gene expression levels of JPH2 and RyR2 were normalized to the GAPDH gene. The mRNA expression levels were calculated by the $2^{-\Delta\Delta Ct}$ method.

To determine levels of expression of JPH2 and RyR2 proteins, infected samples of mouse myocardium were lysed in RIPA buffer. Total protein concentrations were determined using BCA kits (Thermo Fisher Scientific). Precipitated proteins were analyzed with western blotting methodologies.

Ca²⁺ transient measurements

Infected adult cardiomyocytes were incubated with 2 $\mu\text{mol/L}$ fura-2 for 30 min at 37 °C, and then were washed twice with Tyrodes solution containing 1.8 mmol/L CaCl₂. We stimulated cells at 1.0 Hz using field stimulation to evoke Ca²⁺ transient. Levels of intracellular Ca²⁺ were determined by calculation of the 340 to 380 nm (340/380) ratio of Fura-2 fluorescence excited at 510 nm using an IonOptix photometry system (PMT-300, USA). The SR based calcium content in cells was determined by using 10 mM caffeine. Data were collected and analyzed by using SignalAverager Software IonWizard 6.6 (IonOptix) and with all parameters set to manufacture defaults.

Statistical analysis

Data were expressed as the mean value \pm standard error of the mean (SEM). Differences between the treatment groups were evaluated using one-way ANOVA followed by paired or unpaired Student's t tests as appropriate. Differences were considered significant when P values were ≤ 0.05 .

Results

Search of the JPH2 interactome in the Cardiac SR membrane vesicles using LC-MS/MS analysis

To define the functional interactome of JPH2 protein in the heart, we isolated cardiac SR vesicles and performed LC-MS/MS analysis, followed by bioinformatic analysis. The SR vesicles are known to possess junctional sarcoplasmic reticulum-plasmalemma complexes[20, 21], and thus we assessed the presence of JPH2 and RyR2 in the SR vesicles via western blotting. Specific anti-JPH2 and anti-RyR2 antibodies were individually used for the recognition of JPH2 (MW \sim 97 kDa) and RyR2 (\sim 565 kDa; Fig. 1A). Results revealed that JPH2 and RyR2 are present in SR vesicles. Furthermore, the JPH2 immunoprecipitate was pulled-down using anti-JPH2 antibodies with protein A/G plus agarose from SR vesicles and was separated by SDS-PAGE, digested in in-gel trypsin, and underwent LC-MS/MS analysis. JPH2 interacting proteins were approximately 35013 in 13 different target bands chosen by observations from the Coomassie bright blue stain results. Based on previous literature, we listed the important

proteins that were found to interact with JPH2 in Table2. The selected proteins were classified on the Gene ontology website, according to the molecular function, it can be divided into binding protein, catalytic protein, receptor active protein, structural molecule active protein and transport active protein (Fig. 1B). According to the different proteins involved in physiological process, they can be divided into 12 classes, of which most of the proteins involved in cellular physiological movement, followed by some of the local function involved in cell metabolic process, cell developmental process and the others arranged in Fig. 1C. We further construct our version of the JPH2 interaction network among the selected 90 proteins using the STRING tool (<http://string.embl.de/>). By analyzing experimentally confirmed values and the predicted values in a statistically based three-dimensional assessment, we found that some proteins interacted with each other based on their genetic relationships (Fig. 1D). Meanwhile, we carried out additional biologically based validations and network analyses to better understand the dynamics behind the model of their interaction. Although JPH2 and RyR2 proteins had not been found in the most complete three-dimensional model in our computer modeling assessments, the possibility of interactions between them can be hypothesized since their direct homologous proteins can be co-expressed in the same species (Fig. 1E).

JPH2 associates with RyR2 receptors in the Cardiac membrane SR vesicles

We examined the interaction between JPH2 and RyR2 in SR vesicles using co-immunoprecipitation assays. Solubilized proteins from SR vesicles were immunoprecipitated using the anti-JPH2 antibody and subsequently immunoblotted using the anti-RyR2 antibody, RyR2 selectively bound to endogenous JPH2 in SR vesicles (Fig. 2B, left). Similarly, in the reverse co-IP experiments using the anti-RyR2 antibody (Fig. 2A, right), the JPH2 protein specifically bound to RyR2, whereas no specific immunoreaction was observed using an unrelated antibody (Fig. 2A, left and right panels). These results imply that a specific interaction between JPH2 and RyR2 in native cardiac tissue.

We further observed that JPH2 selectively bound to RyR2 using GST pull down assay. The experiments were performed on three GST-fused constructs, including GST-JPH2-N1, GST-JPH2-N2, and GST-JPH2-C [15]. Purified GST or GST-JPH2 fragments fusion proteins were immobilized using glutathione Sepharose 4B affinity beads. Tissue lysates from SR vesicles were then incubated with glutathione Sepharose 4B bound to GST or GST-JPH2 fragments. As shown in Fig. 2B, JPH2-C (aa340-696 containing the C-terminal region of JPH2) selectively bound to RyR2. However, GST alone and GST-JPH2-N1 and GST-JPH2-N2 did not interact with RyR2. Our data indicated that the JPH2-C domain contains the majority of the binding sites for the RyR2 receptor in vitro, and ultimately suggest that this is a preliminary structural requirement for JPH2 to link to RyR2.

Colocalization of JPH2 and RyR2 in adult mouse cardiomyocytes

To determine whether JPH2 and RyR2 proteins were colocalized in cardiomyocytes, we carried out immunofluorescent staining of isolated mouse cardiomyocytes. Figures 3A and 3B indicate that JPH2

and RyR2 maintained the same patterns of striation in singly isolated cardiac cells, even in areas where Z-lines were present in ventricular myocytes (Fig. 3B) or areas with Z-tubules in atrial myocytes (Fig. 3A). Results from controls in which staining with the secondary antibodies were used indicated that co-localization of JPH2 and RyR2 in cardiomyocytes was a valid result (Fig. 3C). Scale bars, 10 μ m.

JPH2 mutation disrupts the interaction between JPH2 and RyR2

To examine whether the mutation in JP2-C disrupted the binding between the two proteins, we applied Co-IP in HEK293 cells transfected RyR2 + JPH2-C or RyR2 + JPH2-Cmut, the expression of RyR2 channel and JPH2 protein in immunoprecipitation complex was detected by western blot. Figures 4 show that compared with HEK293 cells expressing RyR2 + JPH2-C plasmid, the expression of the pulled down RyR2 channels by JPH2 is significantly decreased in HEK293 cells transfected RyR2 + JPH2-C mut plasmids. The results suggest that JPH2 mutation may affect its binding to RyR2 channels.

Knockdown of JPH2 depresses intracellular Ca²⁺ transient

To test whether JPH2 modulated RyR2 receptor function, we used the approach of RNA based interference and recorded levels of intracellular Ca²⁺ transients. After transfection of adenovirus vector with specific siJPH2 through tail vein injection, the levels of JPH2 mRNA (Fig. 5A) and proteins (Fig. 5C, 5D) in adult mouse myocardium infected with Ad-siJP2 were significantly suppressed compared with the control groups (Ad-NC). However, knockdown of JPH2 did not change the mRNA (Fig. 5B) and proteins (Fig. 5E, 5F) of RyR2.

Typical recordings of the intracellular Ca²⁺ transients in infected cardiomyocytes were revealed in Fig. 6A. The amplitude of Ca²⁺ transients was significantly decreased in the treatment of cells transfected JPH2 siRNA (0.33 ± 0.02 , $n = 36$) compared with the control cells (0.52 ± 0.16 , $n = 36$, $P < 0.05$) (Fig. 6C). The resting calcium levels were unchanged in the cardiac myocytes infected with Ad-siJP2 compared with the control cells (1.15 ± 0.26 vs 1.19 ± 0.24 ratio unites, $p = 0.30$, $n = 30$ from 9 heart) (Fig. 6B). We further investigated whether knockdown of JPH2 interfered with the function of the RyR2 receptor. The similar results demonstrated the amplitude of Ca²⁺ transients was significantly decreased in the Ad-siJPH2 treatment group compared with the control group where we used 10 mmol /L caffeine in cell suspension (0.51 ± 0.02 vs 0.87 ± 0.03 ratio unites, $n = 32$ from 9 heart, $P < 0.05$) (Fig. 6D).

Discussion

JPH2 is the cardiac isoform of the junctophilin family and acts as a molecular bridge for signal transduction by anchoring PM and ER/SR membrane systems[9]. In cardiomyocytes, a system of tubules is distributed around the myofibrils and is called diad or peripheral coupling. An association with T-tubules forms by invaginations of the sarcolemmal membrane which is closely juxtaposed with a single terminal cistern of the SR[22]. In the present study, cardiac SR membrane vesicles possessing peripheral

coupling from mice were isolated by differential separation, and specific anti-JPH2 and anti-RyR2 antibodies were recognized JPH2 and RyR2 in the SR vesicles.

JPH2 has been previously suggested to interact with RyR2 and Cav1.2 such as to regulate their gating channel functions[23, 24]. Previous observations suggested that both JPH2 and RyR2 labeling puncta strongly overlapped, and that the amount of JPH2 associated with RyR2 clusters was greatly reduced after JPH2 was manually knocked down[14, 25]. In the present study, the interaction between JPH2 and RyR2 channels can be possibly predicted by LC-MS/MS and biochemical analysis in vitro and in living cells. We used co-immunoprecipitation assays and results suggested that RyR2 was interacting with JPH2 proteins in SR vesicles, and suggested that the majority of both JPH2 and RyR2 proteins were colocalized near Z-lines in adult mouse cardiomyocytes by confocal immunofluorescent imaging analysis. Thus, we provided further evidence that JPH2, a member of the JMC family of proteins found in cardiomyocytes, interacts with RyR2 receptors.

Previous research had predicted that JPHs have a short, C-terminal domain important for anchoring proteins into ER/SR as well as having repeated N-terminal MORN domains which are able to interact with the PM, thereby causing a junctional association of these two membrane systems[9]. Results from a related study indicated that the N-terminal domain of JPH2 is responsible for a physical and functional interaction with small-conductance Ca^{2+} -activated K^+ channels subtype 2 (SK2) in PM[15]. We found that the region of JPH2 (amino acid residues 340–696) interacted with RyR2 in mouse cardiomyocytes. Recent reports have suggested that the N terminus region of JPH2 (amino acid residues 1-565) interacted with RyR2 and Cav1.2, but did not interact with the C terminus region of JPH2 (amino acid residues 566-end), and indicated it was not sufficient to restore Ca^{2+} transients in knocked down JPH2 cardiomyocytes[26]. According to the different cleavage products found in the study compared to our results, we inferred that the overlapping region 340–565 may contain the determinants for the binding between JPH2 and RyR2. Meanwhile, a recent report identified a novel HCM-associated mutation A405S in JPH2, and alters intracellular Ca^{2+} signaling in a pro-hypertrophic manner[27]. We then confirmed the mutation A405S in JPH2 affect its binding with RyR2 channel, indicating that the C terminus of JPH2 proteins was essential for the interaction. In another study, Beavers et al. found that E169K mutation in JPH2 specifically disrupts its binding domain with RyR2 due to perturbed Ca^{2+} handling, indicating residue E169 within a crucial domain of JPH2 that modulates RyR2 channel [28]. E169 residue in JPH2 is located in a flexible 'joining domain' between two MORN domains that attach JPH2 to the sarcolemma[9, 10].

Recent studies have also demonstrated that cardiac-specific knockdown of JPH2 triggers an SR Ca^{2+} leak by directly increasing the probability of RyR2 receptors being open in cardiomyocytes[14, 23, 28]. Moreover, downregulation of JPH2 has been observed in patients with hypertrophic cardiomyopathy, for some rodent based model analyses of hypertrophic cardiomyopathy, overexpression of JPH2 which could correct cardiac function with early stage heart failure, for approaches to inhibition of SR Ca^{2+} leak induced by RyR2[12, 13]. Thus, these results suggest JPH2 could modulate intracellular Ca^{2+} handling

through regulation of RyR2. In the present study, we further confirmed that a siRNA based knockdown of JPH2 resulted in reduced amplitudes of Ca^{2+} transient in cardiomyocytes, but the respective levels of expression of RyR2 mRNA and proteins showed no significant changes in our reports[15]. This result is consistent with previous findings from similarly oriented analyses by authors of this study and other researchers[14, 15, 23, 28], and was a result likely due to decreasing levels of SR Ca^{2+} stores which resulted in an SR Ca^{2+} leak by directly increasing the probability that RyR2 receptors would be open.

To summarize, our data confirm that JPH2 plays a critical role in regulating intracellular calcium level by binding to and modulating RyR2 through its C-terminal domain. Nevertheless, further research is warranted to unequivocally evaluate the specific mechanisms by which JP2 proteins influence RyR2 channel function in vivo to determine the direct link between aberrant ion channel function and cardiac arrhythmias.

Conclusion

In conclusion, we provide more insights into the possible functional regulation of RyR2 channels by the JP2 protein and prove the interaction sites were localized to the C terminus of JPH2 proteins, which consequently plays important roles in maintaining intracellular calcium homeostasis and excitation-contraction coupling.

Abbreviations

RyRs: Ryanodine receptors

ER/SR: endoplasmic/sarcoplasmic reticulum

JPH2/JP2: Junctophilin-2

PM: plasma membrane

MORN: membrane occupation and recognition nexus

VGCC: voltage-gated Ca^{2+} channels

HF: Heart failure

JMC: junctional membrane complex

aa: amino acids

LC-MS/MS: Liquid chromatography-tandem mass spectrometry

IPTG: isopropyl- β -D-thiogalactoside

Declarations

Availability of data and materials

All data generated or analyzed during this study are included in this manuscript.

Acknowledgements

Not applicable.

Funding

This study was funded by National Natural Science Foundation of China (No. 81570311 and 81270248).

Author information

Affiliations

Department of Physiology, School of Basic Medical Sciences, Zhengzhou University, Zhengzhou, 450000, Henan, China

Tianxia Luo, Ningning Yan, Mengru Xu, Fengjuan Dong, Qian Liang, Ying Xing & Hongkun Fan

Contributions

TXL planned the experiments, carried out the functional categorization and network analysis, immunofluorescence stains, CO-IP analysis, GST-pulldown, and wrote the manuscript; MRX, FJD, QL performed the animal experiments, cell culture and real-time PCR; NNY contributed to accomplishing the Ca^{2+} transient measurements; YX and HKF discussed the data and contributed to the conception and design of the research, analysis, and interpretation of data, and revising the article. All authors approved the final manuscript.

Corresponding author

Correspondence to Hongkun Fan

Ethics declarations

Ethics approval and consent to participate

Ethics for animal care followed guidelines from the Committee on the Ethics of Animal Experiments of the University of Zhengzhou, China (No. SYXK-2010-0001). Procedures for experimental use of animals followed guidelines from the National Institutes of Health and Institution.

Consent for publication

Not applicable.

Competing Interests

The authors declare that they have no conflicts of interest.

References

- 1 Nabauer M, Callewaert G, Cleemann L, Morad M: Regulation of calcium release is gated by calcium current, not gating charge, in cardiac myocytes. *Science (New York, NY)* 1989;244:800-803.
- 2 Dulhunty AF: The voltage-activation of contraction in skeletal muscle. *Prog Biophys Mol Biol* 1992;57:181-223.
- 3 Rios E, Pizarro G, Stefani E: Charge movement and the nature of signal transduction in skeletal muscle excitation-contraction coupling. *Annu Rev Physiol* 1992;54:109-133.
- 4 Giannini G, Conti A, Mammarella S, Scrobogna M, Sorrentino V: The ryanodine receptor/calcium channel genes are widely and differentially expressed in murine brain and peripheral tissues. *J Cell Biol* 1995;128:893-904.
- 5 Woo JS, Hwang JH, Ko JK, Kim DH, Ma J, Lee EH: Glutamate at position 227 of junctophilin-2 is involved in binding to TRPC3. *Mol Cell Biochem* 2009;328:25-32.
- 6 Golini L, Chouabe C, Berthier C, Cusimano V, Fornaro M, Bonvallet R, Formoso L, Giacomello E, Jacquemond V, Sorrentino V: Junctophilin 1 and 2 proteins interact with the L-type Ca²⁺ channel dihydropyridine receptors (DHPRs) in skeletal muscle. *J Biol Chem* 2011;286:43717-43725.
- 7 Lee EH, Cherednichenko G, Pessah IN, Allen PD: Functional coupling between TRPC3 and RyR1 regulates the expressions of key triadic proteins. *J Biol Chem* 2006;281:10042-10048.
- 8 Woo JS, Kim DH, Allen PD, Lee EH: TRPC3-interacting triadic proteins in skeletal muscle. *Biochem J* 2008;411:399-405.
- 9 Takeshima H, Komazaki S, Nishi M, Iino M, Kangawa K: Junctophilins: a novel family of junctional membrane complex proteins. *Molecular cell* 2000;6:11-22.
- 10 Garbino A, van Oort RJ, Dixit SS, Landstrom AP, Ackerman MJ, Wehrens XH: Molecular evolution of the junctophilin gene family. *Physiol Genomics* 2009;37:175-186.
- 11 Takeshima H, Hoshijima M, Song LS: Ca²⁺(+) microdomains organized by junctophilins. *Cell Calcium* 2015;58:349-356.
- 12 Landstrom AP, Kellen CA, Dixit SS, van Oort RJ, Garbino A, Weisleder N, Ma J, Wehrens XH, Ackerman MJ: Junctophilin-2 expression silencing causes cardiocyte hypertrophy and abnormal

intracellular calcium-handling. *Circulation Heart failure* 2011;4:214-223.

- 13 Reynolds JO, Quick AP, Wang Q, Beavers DL, Philippen LE, Showell J, Barreto-Torres G, Thuerauf DJ, Doroudgar S, Glembotski CC, Wehrens XH: Junctophilin-2 gene therapy rescues heart failure by normalizing RyR2-mediated Ca(2+) release. *Int J Cardiol* 2016;225:371-380.
- 14 Munro ML, Jayasinghe ID, Wang Q, Quick A, Wang W, Baddeley D, Wehrens XH, Soeller C: Junctophilin-2 in the nanoscale organisation and functional signalling of ryanodine receptor clusters in cardiomyocytes. *J Cell Sci* 2016;129:4388-4398.
- 15 Fan HK, Luo TX, Zhao WD, Mu YH, Yang Y, Guo WJ, Tu HY, Zhang Q: Functional interaction of Junctophilin 2 with small- conductance Ca(2+) -activated potassium channel subtype 2(SK2) in mouse cardiac myocytes. *Acta physiologica (Oxford, England)* 2018;222
- 16 Lee EH, Rho SH, Kwon SJ, Eom SH, Allen PD, Kim DH: N-terminal region of FKBP12 is essential for binding to the skeletal ryanodine receptor. *J Biol Chem* 2004;279:26481-26488.
- 17 Schilling WP, Lindenmayer GE: Voltage-sensitive calcium flux promoted by vesicles in an isolated cardiac sarcolemma preparation. *J Membr Biol* 1984;79:163-173.
- 18 Shevchenko A, Tomas H, Havlis J, Olsen JV, Mann M: In-gel digestion for mass spectrometric characterization of proteins and proteomes. *Nat Protoc* 2006;1:2856-2860.
- 19 Mu YH, Zhao WC, Duan P, Chen Y, Zhao WD, Wang Q, Tu HY, Zhang Q: RyR2 modulates a Ca2+ activated K+ current in mouse cardiac myocytes. *PLoS One* 2014;9:e94905.
- 20 Brandt NR, Caswell AH, Carl SA, Ferguson DG, Brandt T, Brunschwig JP, Bassett AL: Detection and localization of triadin in rat ventricular muscle. *J Membr Biol* 1993;131:219-228.
- 21 Phimister AJ, Lango J, Lee EH, Ernst-Russell MA, Takeshima H, Ma J, Allen PD, Pessah IN: Conformation-dependent stability of junctophilin 1 (JP1) and ryanodine receptor type 1 (RyR1) channel complex is mediated by their hyper-reactive thiols. *J Biol Chem* 2007;282:8667-8677.
- 22 Franzini-Armstrong C: Architecture and regulation of the Ca2+ delivery system in muscle cells. *Appl Physiol Nutr Metab* 2009;34:323-327.
- 23 van Oort RJ, Garbino A, Wang W, Dixit SS, Landstrom AP, Gaur N, De Almeida AC, Skapura DG, Rudy Y, Burns AR, Ackerman MJ, Wehrens XH: Disrupted junctional membrane complexes and hyperactive ryanodine receptors after acute junctophilin knockdown in mice. *Circulation* 2011;123:979-988.
- 24 Li RC, Tao J, Guo YB, Wu HD, Liu RF, Bai Y, Lv ZZ, Luo GZ, Li LL, Wang M, Yang HQ, Gao W, Han QD, Zhang YY, Wang XJ, Xu M, Wang SQ: In vivo suppression of microRNA-24 prevents the transition toward decompensated hypertrophy in aortic-constricted mice. *Circ Res* 2013;112:601-605.

- 25 Jayasinghe ID, Baddeley D, Kong CH, Wehrens XH, Cannell MB, Soeller C: Nanoscale organization of junctophilin-2 and ryanodine receptors within peripheral couplings of rat ventricular cardiomyocytes. *Biophys J* 2012;102:L19-21.
- 26 Guo A, Hall D, Zhang C, Peng T, Miller JD, Kutschke W, Grueter CE, Johnson FL, Lin RZ, Song LS: Molecular Determinants of Calpain-dependent Cleavage of Junctophilin-2 Protein in Cardiomyocytes. *J Biol Chem* 2015;290:17946-17955.
- 27 Quick AP, Landstrom AP, Wang Q, Beavers DL, Reynolds JO, Barreto-Torres G, Tran V, Showell J, Philippen LE, Morris SA, Skapura D, Bos JM, Pedersen SE, Pautler RG, Ackerman MJ, Wehrens XH: Novel junctophilin-2 mutation A405S is associated with basal septal hypertrophy and diastolic dysfunction. *JACC Basic Transl Sci* 2017;2:56-67.
- 28 Beavers DL, Wang W, Ather S, Voigt N, Garbino A, Dixit SS, Landstrom AP, Li N, Wang Q, Olivotto I, Dobrev D, Ackerman MJ, Wehrens XHT: Mutation E169K in junctophilin-2 causes atrial fibrillation due to impaired RyR2 stabilization. *Journal of the American College of Cardiology* 2013;62:2010-2019.

Tables

Table 1 Primers used to amplify JPH2, RyR2 and GAPDH

Gene name sequence

JPH2

Forward: 5'-CTGGCTATCCATTTGTTACCT-3',

Reverse: 5'-GTTTTAGGTCCGAAGTCCCAT-3';

RyR2

Forward: 5'-GAATTCATCATGGATACTCTACC-3',

Reverse: 5'-GTCATGCACATTATCTTCTGCAT-3';

GAPDH

Forward: 5'-GGTTGTCTCCTGCGACTTCA-3',

Reverse: 5'-TGGTCCAGGGTTTCTTACTCC-3'.

Table 2 JPH2 interactome proteins

Proteins	Accession	MW [kDa]	calc. pI
Myosin-6	Q02566	223.4	5.73
SERCA2A	O55143-2	109.7	5.36
ADP/ATP translocase	P48962	32.9	9.76
Sodium/potassium-transporting ATPase subunit alpha-1	Q8VDN2	112.9	5.45
Ryanodine receptor 2	E9Q401	564.5	6.09
Histidine rich calcium binding protein	G5E8J6	85.1	4.63
Sodium/potassium-transporting ATPase subunit alpha-2	D3YYN7	103.5	5.44
Laminin subunit alpha-2	Q60675	343.6	6.09
Laminin subunit gamma-1	F8VQJ3	177.1	5.19
Phosphate carrier protein	Q8VEM8	39.6	9.26
Sodium/potassium-transporting ATPase subunit alpha-3	Q6PIC6	111.6	5.41
Creatine kinase S-type	Q6P8J7	47.4	8.4
Fibrillin-1	A2AQ53	312.1	4.92
Sodium/calcium exchanger 1	G3X9J1	108	4.98
Voltage-dependent anion-selective channel protein 2	G3UX26	30.4	7.58
Apoptosis-inducing factor 1	B1AU25	66.1	9.11
Myosin-binding protein C	E9Q9T8	141.2	6.60
Gap junction alpha-1 protein	P23242	43	8.76
Sarcalumenin	Q7TQ48	99.1	4.46
Clathrin	Q68FD5	191.4	9.61
Dysferlin	E9QL12	237	5.6
Cleft lip and palate transmembrane protein 1 homolog	Q8VBZ3	75.2	6.3
Isoform 3 of Striated muscle-specific serine/threonine-protein kinase	Q62407-3	262.7	7.78
Integrin	G3X9Q1	124.5	5.74
Junctophilin-2	Q9ET78	74.6	8.16
Endoplasmin	P08113	92.4	4.82

Caveolin-1		P49817	20.5	6.02
Annexin		P14824	75.8	5.5
Voltage-dependent channel	L-type calcium	Q01815-3	210.7	6.65
AFG3-like protein 2		Q8JZQ2	89.5	8.60
Ras-related protein Rab-12		P35283	27.3	8.41
SerpinH1		P19324	46.5	8.82
Cation-independent phosphate receptor	mannose-6-	Q07113	273.6	5.71
glucose-regulated protein		P20029	72.4	5.16
Secretory carrier-associated membrane protein		Q3TSA8	32.3	8.53
Autophagy 9-like 1 protein		Q3ZQA4	94.4	6.64
Murinoglobulin-1		P28665	165.2	6.42
Calnexin		P35564	67.2	4.64
Cardiomyopathy-associated protein 5		E9QLJ0	405.3	4.74
ER lumen protein retaining recepto		D3YU99	15.9	8.29
Moesin		P26041	67.6	6.6
Reticulocalbin-2		Q8BP92	37.2	4.42
Ephrin-B1		P52795	37.8	9.03
Actin		P60710	41.7	5.48
Sialoadhesin		Q62230	182.9	6.67
Calsequestrin-2		O09161	48.1	4.27
Voltage-dependent anion-selective channel protein 2		G3UX26	30.4	7.58
Desmoplakin		E9Q557	332.7	6.8
Cadherin-13		Q9WTR5	78.1	5.12
ER membrane protein complex		Q8C7X2	111.5	7.43
Nebulette		B7ZCI2	115.9	8.51

Calpastatin	Q8CE80	81.4	5.36
A-kinase anchor protein 1	O08715	92.1	5.02
Zinc-binding alcohol dehydrogenase domain-containing protein 2	Q8BGC4	40.5	7.42
Alpha-2-macroglobulin receptor-associated protein	F6WMD1	18.3	8.32
Serine/threonine-protein kinase	Q6P9R2	58.2	4.63
Cadherin-5	P55284	87.8	5.3
Alpha-centractin	P61164	42.6	6.64
Muscle-related coiled-coil protein	A2AMM0	41	8.65
Reticulon-4	Q99P72-3	114.02	4.68
Calcium/calmodulin-dependent protein kinase type II	F6WHR9	19.9	7.46
Tight junction protein	Q9Z0U1	131.2	6.79
Catenin	P26231	100	6.23
Endoplasmic reticulum aminopeptidase	Q9EQH2	106.5	6.2
Nck-associated protein	P28660	128.7	6.62
Junction plakoglobin	Q02257	81.7	6.14
Plakophilin 2	Q9CQ73	88	9.33
Sarcolemmal membrane-associated protein	F6UV57	50.2	4.87
cardiomyopathy-associated protein5	Q70KF4	412.8	4.75
Transient receptor potential cation channel	Q5KTC0	172.1	7.56
Butyrophilin-like protein 9	Q8BJE2	60.5	6.42
Vimentin	P20152	53.7	5.12
EH domain-containing protein 2	Q8BH64	61.1	6.51
	P58390	60.6	6.83
small conductance calcium-activated channel member			
2			
Chloride channel CLIC-like protein 1	Q99LI2	60.6	5.68

Tyrosine-protein kinas	Q04736	60.6	6.64
Desmin	P31001	53.5	5.27
Atrial natriuretic peptide receptor 3	P70180	59.8	7.06
Beta-2-syntrophin	Q61235	56.3	8.69
Paraplegin	F6W695	27.5	7.62
Calcitonin receptor	Q60755	62.4	8.43
Calcium/calmodulin-dependent protein kinase type II	Q6PHZ2-2	54.1	7.12
Neuroplastin	H3BIX4	24.4	6.1
Protein FAM134C	Q9CQV4	51.6	4.97
Clusterin	Q06890	51.6	5.67
Synapse-associated protein 1	Q9D5V6	41.3	4.54
Sarcoplasmic/endoplasmic reticulum calcium ATPase 2	J3KMM5	109.7	5.34
Na(+)/H(+)exchange regulatory cofactor	P70441	38.6	5.90
Isoform Gnas-3 of Guanine nucleotide-binding protein G(s)	P63094-3	41.8	5.30
Flotillin-1	O08917	47.5	7.15
Flotillin-2	Q60634	47	5.20

Figures

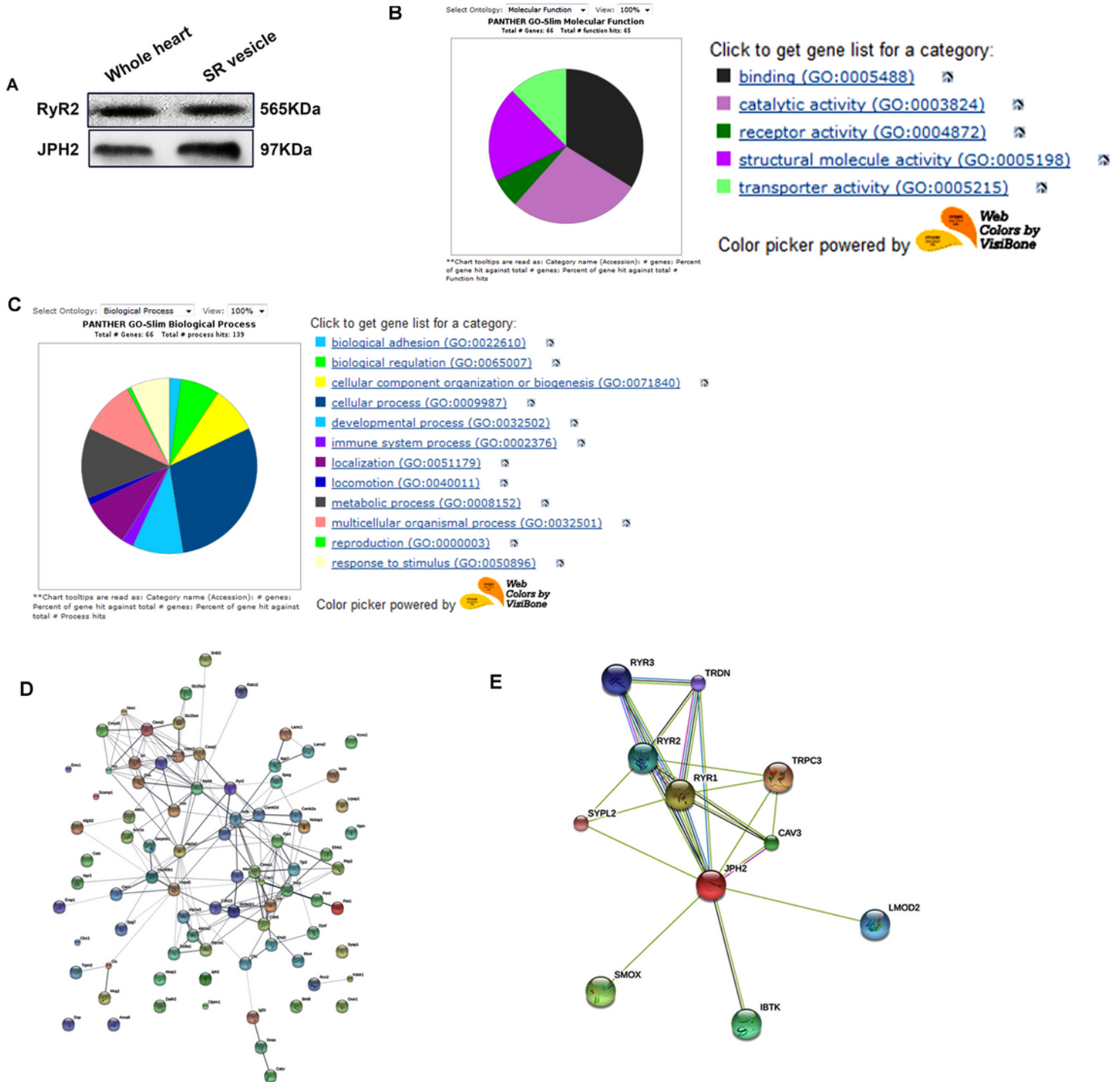


Figure 1

RyR2 is JPH2 interactome in the Cardiac SR membrane vesicles. A. The expression levels of JPH2 and RyR2 were tested in heart tissue and SR vesicles from mouse by western blot analysis. B. The electrophoretogram of JPH2 immunoprecipitate. 13 different target bands were selected by observations from the Coomassie bright blue stain results. C. The selected proteins were classified by molecular function on the Gene ontology website. D. The proteins were classified by biological process. E. 90

proteins were selected to construct JPH2 interaction network using the STRING tool, no interactions were noted between JPH2 and RyR2. F. The possibility of interactions between JPH2 and RyR2 can be hypothesized since their direct homologous proteins can be co-expressed in the same species.

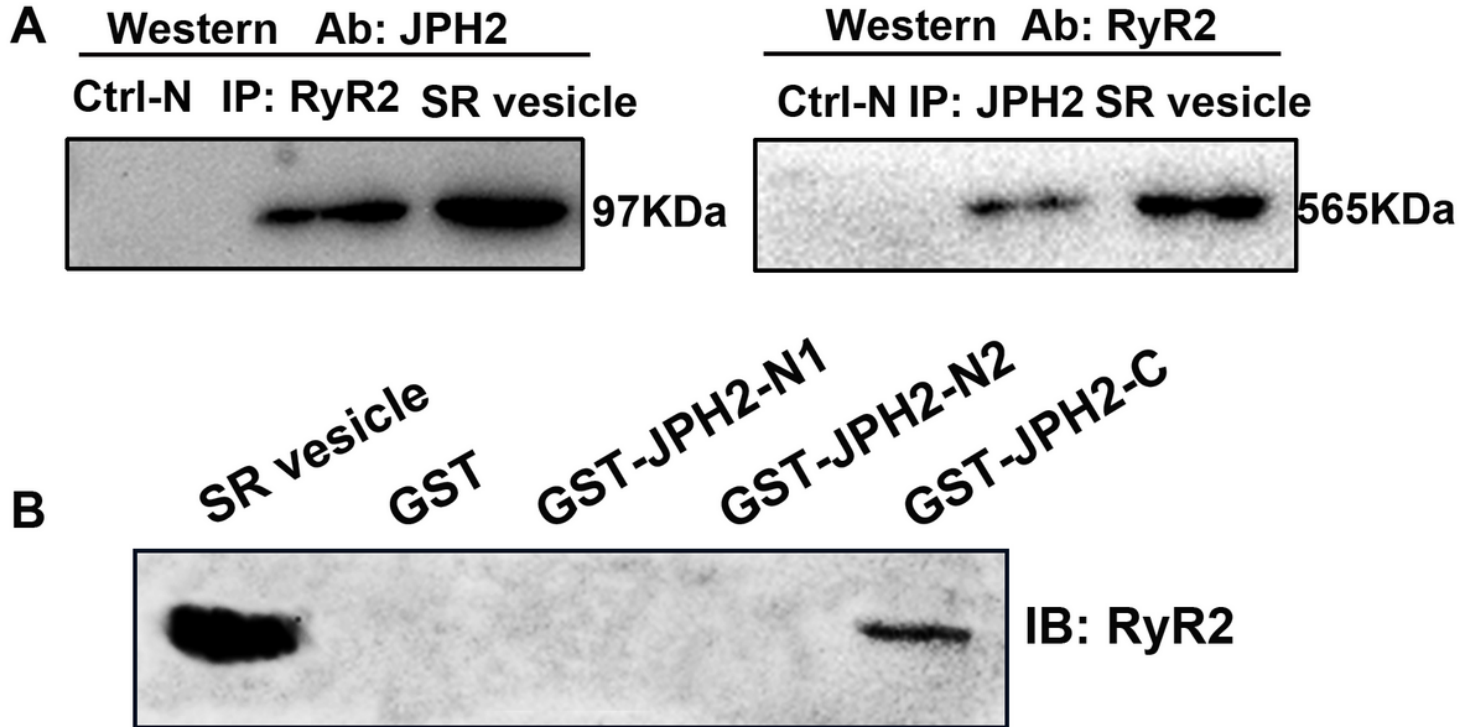


Figure 2

Interaction between JPH2 and RyR2 in isolated cardiac SR membrane vesicles. A. SR vesicles were solubilized and subjected to IP with antibodies to RyR2 or JPH2. The soluble proteins extracted from cardiac SR vesicles were used as positive control, and Ctrl-N was negative control using a non-immobilized gel. B. Purified GST or GST-JPH2 fragment fusion proteins containing GST-JPH2-N1, GST-JPH2-N2 and GST-JPH2-C were immobilized and detected with anti-RyR2 antibody using GST pull down assay.

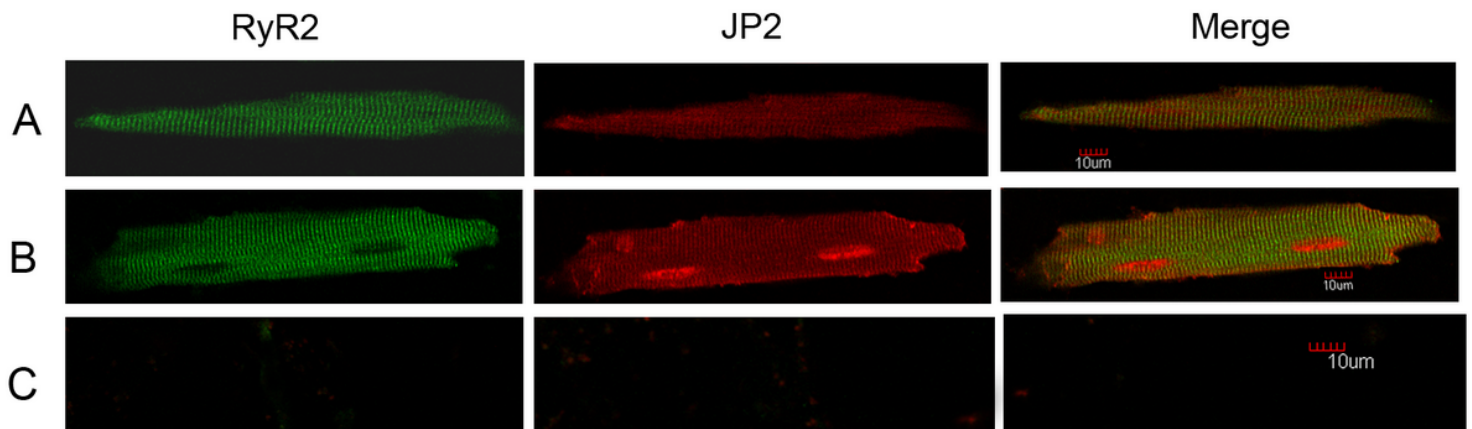


Figure 3

Co-localization of JPH2 and RyR2 in mouse cardiomyocytes. Immunofluorescent staining showed dual immunolabelling of JPH2 (red) with RyR2 (green) in single isolated atrial (A) and ventricular (B) myocytes. C. Negative control experiments (Control) were performed with the secondary antibodies in atria myocytes (Scale bars, 10 μ m).

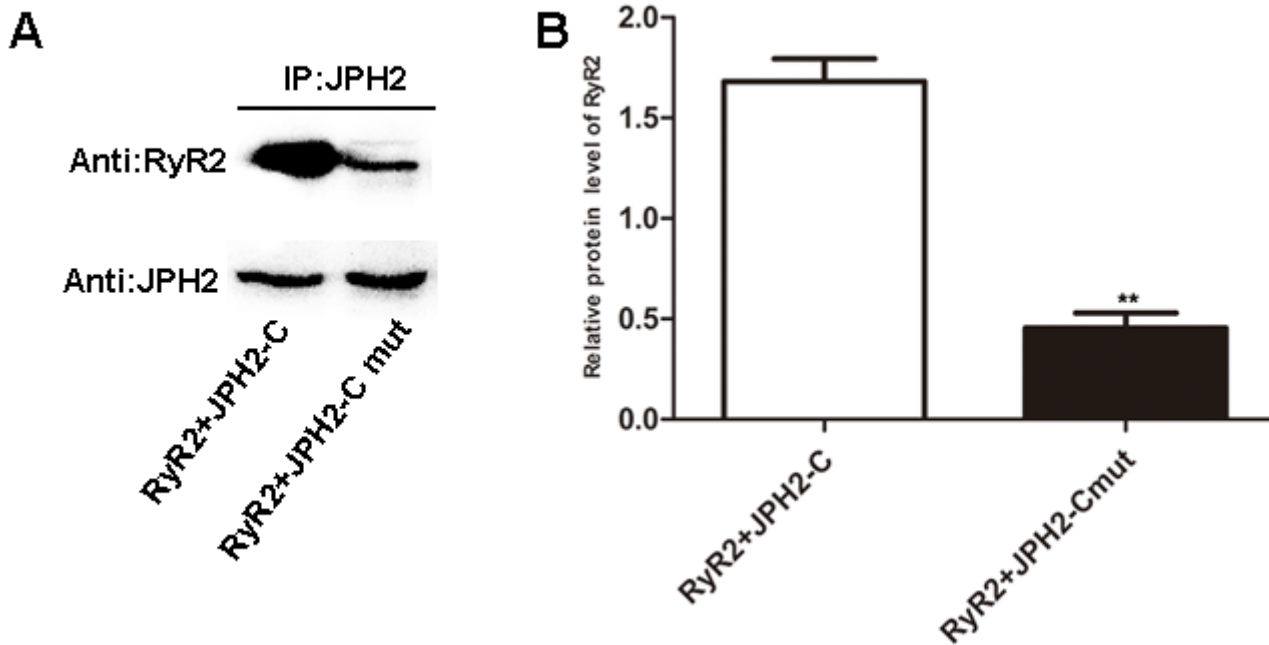


Figure 4

JPH2 mutation decrease its binding with RyR2 channel. A. Protein precipitated (IP) with JPH2 antibody from HEK293 cells transfected with RyR2+JPH2-C or RyR2+JPH2-Cmut plasmids was detected by western blot using JPH2 antibody and RyR2 antibody respectively. B. Relative protein level of RyR2 channel (normalized to immunoprecipitation JPH2) (** P < 0.01).

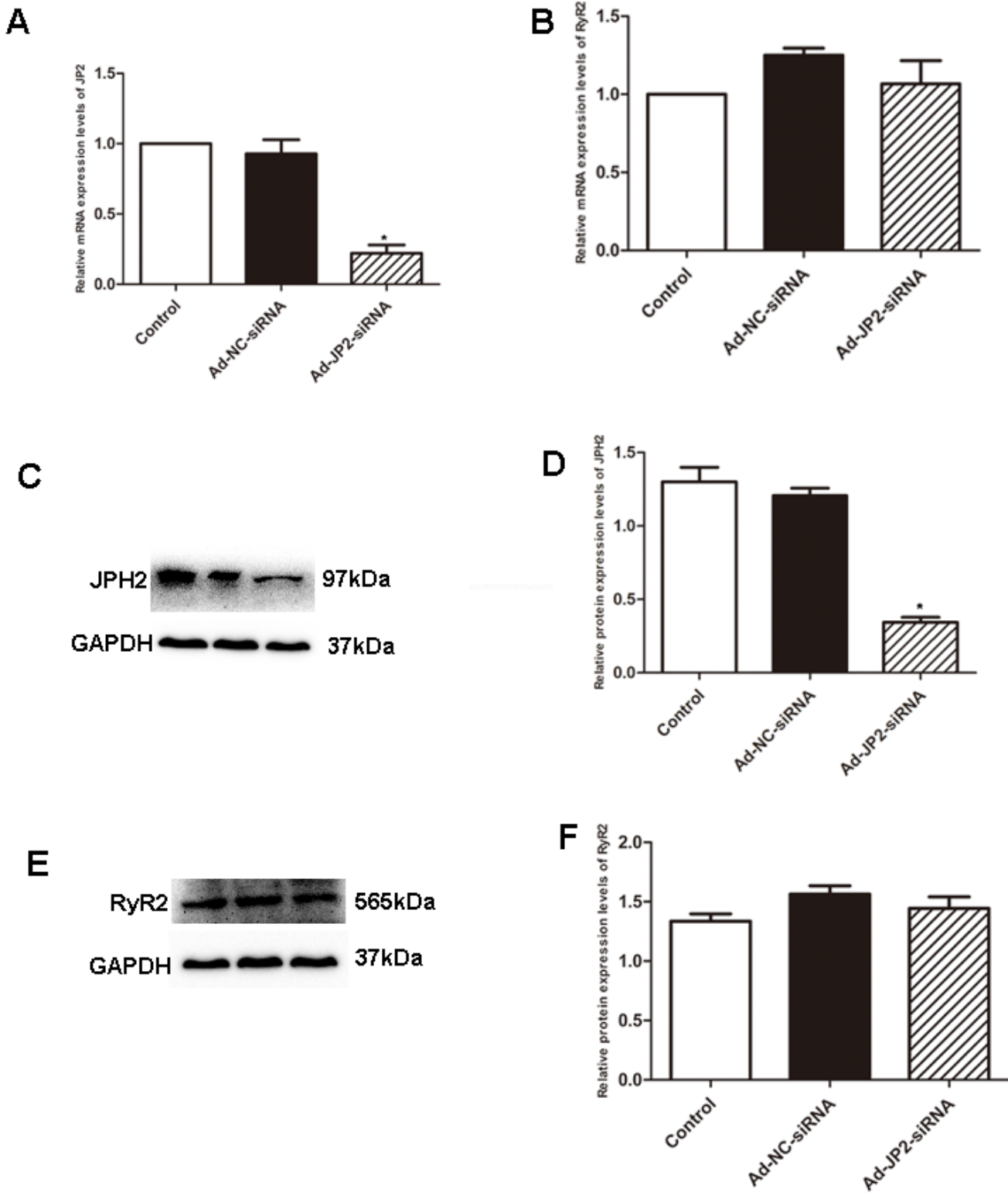


Figure 5

Knockdown of JPH2 did not change the expression of RyR2. A. The bar graphs show significant decrease in JPH2 mRNA of myocardium infected by adenovirus vector with specific JPH2 siRNA (Ad-siJPH2), compared with control groups. B. The bar graphs show RyR2 mRNA did not change in myocardium with different treatments. C. Western blotting analysis of JPH2 expression in different treatments. D. The bar graphs show significant downregulation of JPH2 protein expression after infection of JPH2 siRNA. E. A

representative western blotting analysis showing RyR2 expression in myocardium with different treatments. F. The bar graphs show no significant change of RyR2 mRNA expression after infection of JPH2 siRNA. Error bars represent \pm SEM; (*) $P < .05$ vs control group; Student's t-test.

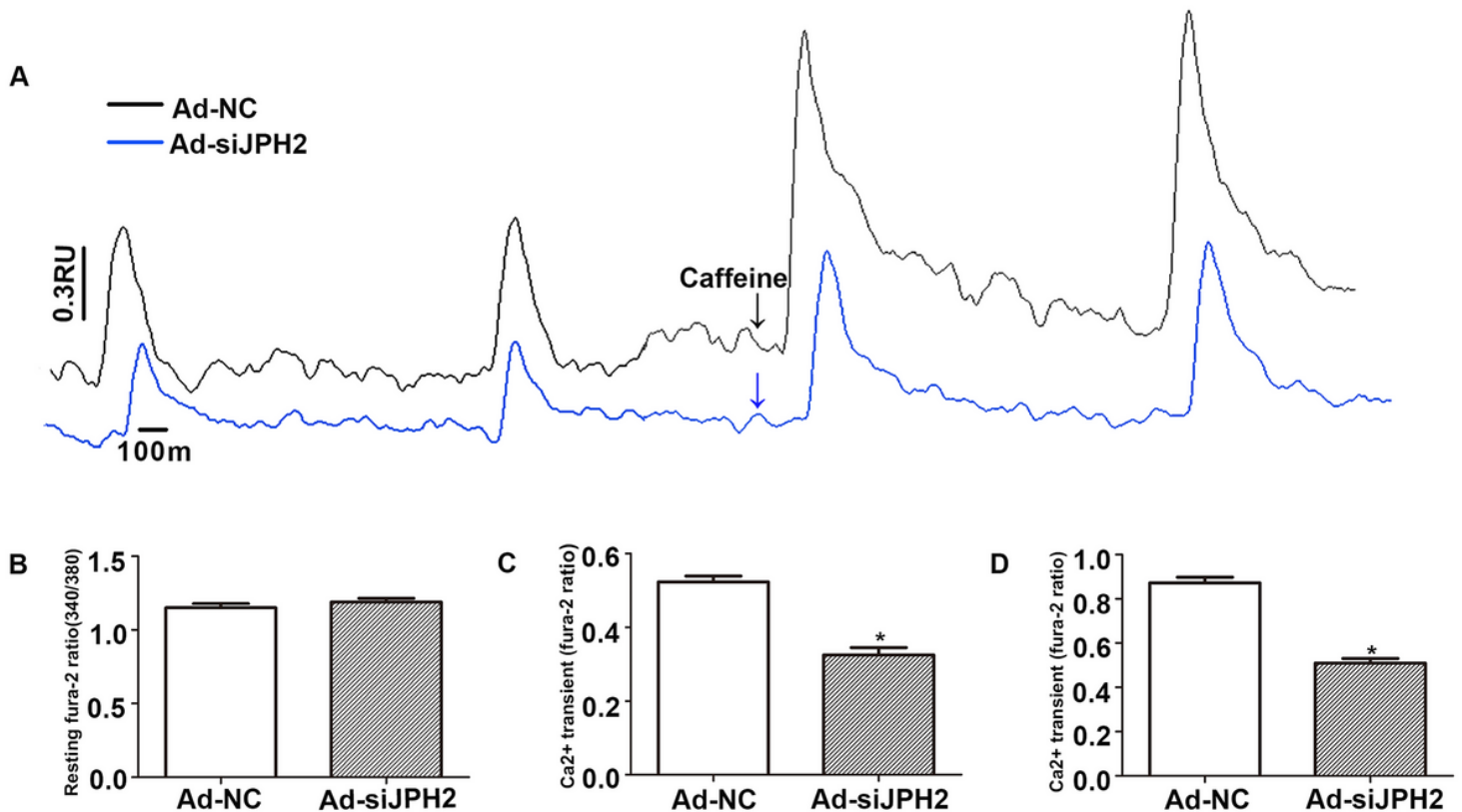


Figure 6

Knockdown of JPH2 depresses Ca²⁺ transient in mouse cardiomyocytes. A. The curves of the Ca²⁺ transient of Fura-2 loaded adult mouse cardiac myocytes. The black curve represents the negative control (Ad-NC), the blue curve is cells transfected by adenovirus vector with specific JPH2 siRNA (Ad-siJPH2). B. The bar graphs of resting fura-2 ratio in Ad-siJPH2 infected mouse cardiac myocytes (n=30 per group). C. The bar graphs of the amplitude of the [Ca²⁺]_i transient in Ad-siJPH2 infected mouse cardiac myocytes (n=36 per group). D. The bar graphs of Ca²⁺ transients elicited by application of 10mM caffeine (n=32 per group). Error bars represent \pm SEM; (*) $P < .05$ vs control group; Student's t-test.

Supplementary Files

This is a list of supplementary files associated with this preprint. Click to download.

- [GraphicalAbstract.jpg](#)